

**2013 NDIA GROUND VEHICLE SYSTEMS ENGINEERING AND TECHNOLOGY  
SYMPOSIUM  
POWER & MOBILITY (P&M) MINI-SYMPOSIUM  
AUGUST 21-22, 2013 - TROY, MICHIGAN**

**PACK LEVEL PERFORMANCE RESULTS FOR A  
UNIVERSAL LITHIUM-BASED BATTERY MANAGEMENT SYSTEM**

**Bruce Pilvelait  
Carlos Rentel  
William Finger  
David Fogg**  
Creare Inc.  
Hanover, NH

**Gregory L. Plett**  
University of Colorado  
Colorado Springs, CO  
**Anthony Knakal**  
Navitas Advanced Solutions Group  
Ann Arbor, MI

**ABSTRACT**

*This paper describes the development of and tests performed on a Battery Management System (BMS) that was developed for lithium ion based cell chemistries. The BMS follows a universal architecture developed to support multiple chemistries. It estimates and reports the State of Charge (SOC), State of Health (SOH), State of Life (SOL), and Power Availability of the battery pack. The BMS also reports current, cell voltages, and temperatures. Additionally, the BMS performs active and passive cell balancing and fault protection via solid state circuit breakers. The BMS package conforms to military requirements, including an operational temperature range between -55°C and +70°C, and provides a Controller Area Network (CAN) interface. Algorithm accuracy performance was quantified in the laboratory. The BMS consistently demonstrated accuracies within 5% SOC in a software upgradeable, low cost package. Currently we are performing field tests on a U.S. Army ground combat vehicle.*

**INTRODUCTION**

Lithium-based batteries provide excellent capacity and power performance. However, they must be carefully managed to enable these performance advantages in a safe and optimum manner. Our objective is to enable the safe and optimum incorporation of lithium-based packs into vehicle battery systems. We have achieved this objective by developing a Universal Lithium-based Battery Management System (BMS) that closely monitors and controls lithium-based battery packs of any chemistry type. Our BMS is capable of estimating and reporting the State of Charge (SOC), State of Health (SOH), State of Life (SOL), Power Availability (PA), pack current, cell voltages, and temperature. It provides two levels of protection against over-voltage, under-voltage, over-current, and over-temperature.

Additionally, the BMS is capable of passive and active cell balancing. In what follows we first describe the BMS in more detail. Then we present the most important laboratory tests results, followed by our plans for the upcoming field tests.

**SYSTEM DESCRIPTION**

Figure 1 illustrates our BMS concept [1], [2]. In this configuration the BMS has eight channels, each capable of handling a number of cells connected in parallel (super-cell). In this embodiment, each channel handles three 20Ah lithium iron phosphate cells connected in parallel. The Master Central Unit is a TI TMS320F28335 DSP, which processes the pack current, super-cell voltages, and temperature measurements to perform the estimation, protection, and cell balancing functions, among other auxiliary tasks.

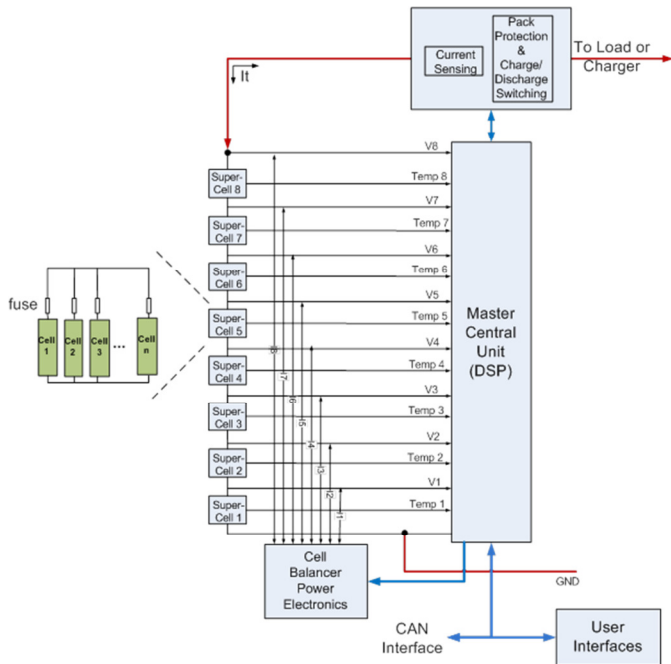


Figure 1. Lithium-based BMS functional block diagram.

**Requirements**

The Universal BMS aims to make possible the use of the latest breed of lithium-based battery packs. The most important requirements are:

- SOC accuracy of 5% or better.
- Report SOH, SOL.
- Report PA in the next 2 seconds and 15 seconds.
- Battle override mode triggered via Controller Area Network (CAN).
- Universal architecture.
- Safety features, such as over-current and over-voltage protection.
- Tare power less than 2W.
- Temperature range from -55°C to +70°C without performance degradation.

**Protection and Safety Features**

The BMS continuously monitors the state of the battery pack and ensures its operational limits are respected. The BMS provides the following protection features: a) over-charge. b) over-discharge, c) over-current, d) over-/under-voltage, e) active and passive cell balancing, and f) thermal limits. The BMS operates in two protection modes: Standard mode and Battle Override mode. The protection thresholds in Battle Override mode are wider to allow a military crew to use the battery pack to its limits disregarding the health or life of the battery, but maintaining safe operation. The Standard mode has narrower protection limits that ensure safe operation and, additionally, the health and life of the battery. If any of the thresholds are exceeded, the BMS commands the positive-side and negative-side solid state circuit breakers to open. Each solid state circuit breaker is comprised of a number of MOSFETs in parallel. All protection thresholds are programmable via CAN. Over-current and over-charge are defined by an instantaneous current threshold and a current time windowed integration threshold respectively. For instance, the BMS can be programmed to open the circuit breakers immediately if the discharging current exceeds 500A. During discharge operations the windowed integration approach prevents the BMS from faulting if extremely short duration current spikes are detected as the load changes rapidly. For example, configuring the BMS to fault if the discharge rate exceeds 900 Coulombs over a window of 2 seconds accommodates continuous discharge currents up to 450A. Short duration spikes above 450A are allowable (e.g., 750A for 0.1 seconds) provided the total integrated charged over the running 2 second window never exceeds the 900 Coulomb threshold. Currents larger than 450A may be limited depending on the load profile.

### Communications and User Interface

The BMS must communicate with other vehicle controllers and computers via CAN. CAN communication is used to report all estimated and measured variables of the pack. Our BMS reports in graphical and tabular form to a Graphical User Interface (GUI) running on a Windows PC. We are able to program, calibrate, turn cell balancing on and off, change protection mode (i.e., Standard or Battle Override), and download and upload parameters and models of the pack via this GUI. The GUI reports the super-cell voltage; pack current; pack and super-cell temperature; and pack and super-cell SOC, SOH, SOL, and PA. Internal resistance of every super-cell is also reported along with fault and error types either in Standard or Battle Override mode. The GUI application continuously logs the data received from the BMS via CAN at a rate of 10Hz.

### Package

The BMS has been designed to fit in a NATO standard 6T pack. Figure 2 shows the 6T pack's external dimensions and a 6T pack. The prototype pack is a +26.4VDC and 60Ah nominal pack, comprised of 24 prismatic lithium iron phosphate 20Ah cells connected in an 8-series 3-parallel (8S3P) configuration. This pack has the BMS and circuit breakers electronic assemblies as shown in Figure 3. Figure 3 also shows the actual BMS electronic assembly. This electronic assembly implements all the functionality depicted in Figure 1, including active cell balancing.

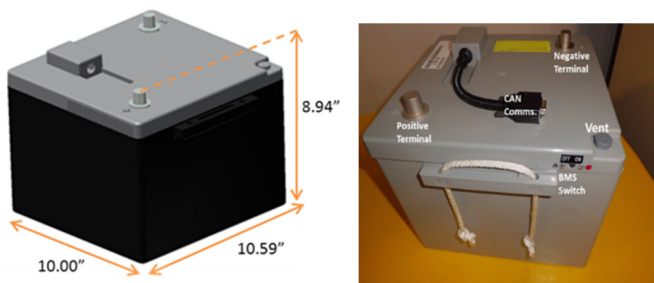


Figure 2. 6T pack's dimensions and prototype.

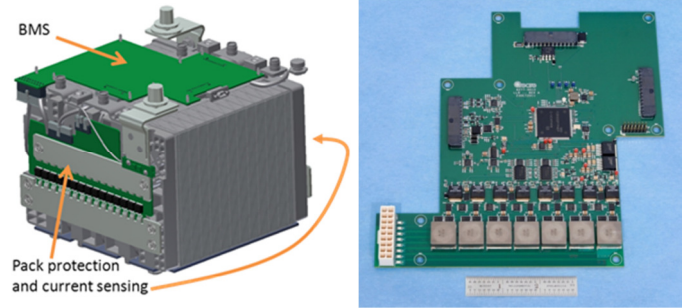


Figure 3. BMS electronic assembly.

### Algorithms

Accuracy, robustness, and simplicity are important features in achieving a practical BMS system. In the following paragraphs, we describe the five algorithms included in the BMS.

**State of Charge:** The SOC algorithm uses a cell model based on an equivalent electrical circuit. The parameters of this model are obtained with off-line tests, before downloading to the BMS's DSP via the GUI and CAN interface. Every lithium-based chemistry variant has its own particular model parameter values, but our model structure remains the same. This latter feature makes the universality of our BMS possible.

The SOC algorithm estimates SOC from both cell terminal voltage and current measurement. The discrete-time cell model is called The Enhanced Self-Correcting model [3]. Its general structure is:

$$SOC(k) = f(I(k), SOC(k - 1), T, \vec{\theta}) \quad (1a)$$

$$\hat{V}(k) = h(I(k), SOC(k - 1), x(k - 1), T, \vec{\beta}) \quad (1b)$$

$$x(k) = g(I(k), x(k - 1), T, \vec{\gamma}) \quad (1c)$$

In this model,  $SOC(k)$  and  $\hat{V}(k)$  are the estimated SOC and estimated terminal voltage at the  $k^{th}$  sampled time (sample frequency is 1 Hz in the developed prototype). Functions  $f()$  and  $h()$  relate previous estimation of SOC (i.e.,  $SOC(k - 1)$ ) and current  $I(k - 1)$ , to present

estimated SOC (i.e.,  $SOC(k)$ ) and terminal voltage (i.e.,  $\hat{V}(k)$ ), respectively; these functions are referred to as process and output functions. Both functions depend on the latest current measurement (i.e.,  $I(k)$ ), previous estimates of SOC (i.e.,  $SOC(k-1)$ ), temperature ( $T$ ), and the parameter-vectors  $\vec{\theta}$  and  $\vec{\beta}$  that are computed off-line, and are updated online as the cell ages.  $\vec{\theta}$  and  $\vec{\beta}$  have elements that include maximum cell capacity, internal resistance, and capacitance of the cell, and their values depend on the specific lithium chemistry.

Functionally, the model in equation (1) is used to estimate SOC by using current, terminal voltage, and temperature measurements. The estimation of SOC based on current is performed by the  $f()$  function, and the fine tuning of this SOC estimation is obtained by adding (or subtracting) a value dependent on the error between the estimated and measured terminal voltage.

The approach is unique and simple, and has shown accuracies within 5% error with respect to true SOC. Continuous parameter value updates are necessary to keep the model accurate as the battery pack ages. The most critical model parameters, such as internal resistance and maximum cell and pack capacity, can be automatically updated on-line by the BMS as the pack ages.

State of Health: The SOH algorithm is based on internal resistance. As internal resistance increases, the ability of the pack to deliver power diminishes. We say that “SOH = 100%” implies the pack is at its peak healthy condition, which implies its internal resistance value equals the nominal resistance when the pack is new. Alternatively, “SOH = 0%” implies a pack is in an unacceptable health condition and should be replaced. In this embodiment, the “SOH = 0%” threshold is specified to be the point at which the internal resistance of the pack reaches 1.5 times its

nominal internal resistance when the pack is new. For instance, the cells used for this testing have an internal resistance at room temperature approximately equal to  $2\text{m}\Omega$  when new. The cell will reach 0% SOH when this resistance is estimated to be  $3\text{m}\Omega$  (or  $1.5 \times 2\text{m}\Omega$ ). The estimation of internal resistance takes into account temperature, and the measurements are filtered with a first-order filter.

State of Life: The SOL algorithm is based on the pack’s maximum capacity. A pack is said to be at its 100% SOL when its maximum capacity is equal to the nominal capacity of the pack when new. A pack is said to have reached 0% SOL when its maximum capacity reaches a percentage, less than 100%, of the nominal capacity when the pack was new. Typically this percentage is taken to be 80%. For instance, this pack has a nominal maximum capacity of 60Ah. This capacity will hold for some time depending on how the pack is used. As the pack ages, its ability to hold charge decreases. When the pack can only hold a maximum charge of 48Ah (i.e., 80% of 60Ah), it is specified to have reached the end of its life (i.e., SOL = 0%). This and all other thresholds in the BMS can be changed to adapt to a particular scenario or application.

Analogous to the SOH algorithm, SOL is expected to change slowly, with time constants on the order of months. To minimize fluctuations in the maximum capacity estimates due to statistical outliers, each individual capacity measurement opportunity is processed through a filter.

Power Availability: For most SOC conditions the maximum power the pack can deliver is determined by the PA algorithm. The load will likely have a minimum voltage requirement which needs to be respected in practice. If the battery pack terminal voltage is not allowed to go below a minimum pre-defined voltage (e.g., the pack under-voltage protection threshold), then the PA

algorithm will take this into consideration. The PA algorithm is updated at a rate of 1Hz when the pack is being discharged, and it predicts the power available in discrete intervals.

**Cell Balancing:** Cell balancing is a very important feature in any battery pack comprised of multiple rechargeable cells connected in series. The main goal is to maximize the useful pack capacity and ensure the maximum and minimum allowable cell voltages are respected for safety. Cell balancing can be classified in two ways depending on how the energy is transferred or controlled: a) active balancing via energy transfer, and b) passive balancing via energy dissipation through high power resistors [4]. It can also be classified depending on the variable being balanced, typically: a) voltage-based cell balancing, and b) SOC-based cell balancing. In voltage-based cell balancing, the goal is to make sure all cells have the same voltage in all situations.

Our BMS is designed to provide voltage-based passive balancing and active balancing. Passive balancing is triggered manually when balancing of the pack is deemed necessary. Passive balancing is meant to be used when the pack is not actively being charged or discharged. Once the user triggers passive balancing, via the provided GUI, the BMS opens the circuit-breakers to ensure an unloaded condition, and the process continues automatically until all cells are voltage balanced. Active balancing operates on-line continuously, unless a user turns it off via the GUI.

Figure 4 shows the main active balancing principle. The building block circuit of the active cell balancing circuit is referred to as a dual-cell balancer, and it is based on transferring charge between two cells using an inductor as energy storage element in a two-step process. The inductive cell balancing approach can be scaled to any number of cells in series, as depicted in Figure 4 for the case of four cells. The blocks

represent the dual cell balancers, which are controlled by the BMS via the electronic switches (not shown) to transfer energy from cell to cell. Transferring energy from non-adjacent cells can be done in several ways. For instance, if the cell balancing algorithm determines that energy needs to be transferred from cell V3 to cell V0, then one possibility is to transfer from V1 to V0, then from V2 to V1, and finally from V3 to V2 sequentially. Concurrent energy transfer is also possible; for instance, energy transfer from V3 to V2 can happen at the same time as energy transfer from V2 to V1, and from V1 to V0; this will effectively transfer energy from V3 to V0 through all the intermediate cells concurrently.

The latter approach will speed up cell balancing. An example of a concurrent energy transfer is depicted in Figure 4 by the solid and dotted arrows. The energy transfer rate can be adjusted using a different switching frequency (lower frequency higher energy transfer) and/or different inductor sizes.

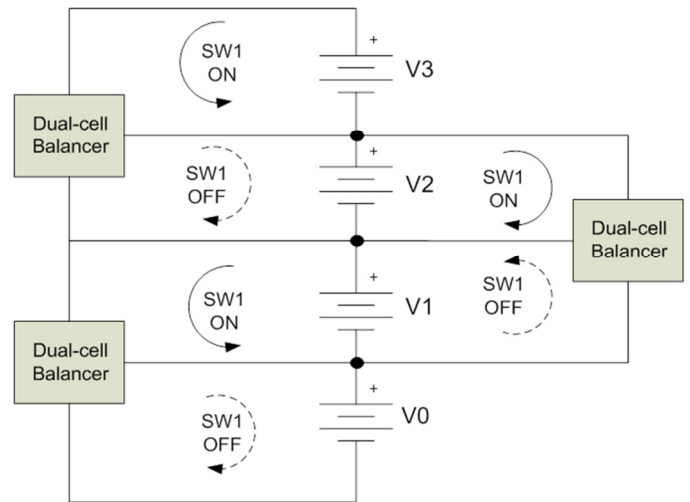


Figure 4. Active cell balancing architecture.

**LABORATORY TEST RESULTS**

The BMS was evaluated in the laboratory prior to its field deployment. Here we present results of the laboratory tests for different functions.

**Protection Performance Tests**

To avoid creating hazardous conditions in the laboratory, pack protection functionality was verified by simulating conditions exceeding the corresponding thresholds. For safety, this testing was achieved by using power supplies rather than actual cells. Control signals simulating current, voltage, and temperature over-limit conditions were applied to the respective BMS sensing lines. The BMS response was then monitored and verified to act correctly by opening the circuit-breakers between the pack and the load. The BMS was also verified to change to either mode of operation when commanded via CAN; that is, the BMS changed its safety limits between standard and battle override mode when commanded.

Table 1 lists Battle Override limits used in our laboratory tests. These can be set to higher values once the pack is deployed. For brevity, we present results for Battle Override only since the Standard mode results showed the same performance; only the values of the thresholds differ.

Table 1. Safety thresholds during laboratory tests	
Safety parameter	Battle Override threshold
Over-voltage	+4.20VDC
Under-voltage	+1.65VDC
Instantaneous over-current	±11A
Over-charge	$\int_{t-60s}^t I dt \geq 280$ Coulombs

Figure 5 and Figure 6 demonstrate fault activation for over-voltage and under-voltage. For the over-voltage case (Figure 5), the voltage is manually increased until it exceeds the over-voltage criterion (> 4.20V), at which point the software identifies the fault with the unique over-voltage fault code (4) and opens the circuit breakers. Opening the circuit breakers decouples the battery from the load electronics, thereby protecting the cells from failure. For the under-voltage case (Figure 6), the voltage is manually decreased until the under-voltage criterion (< 1.65V) is reached, triggering a fault event identified by code (6). Once again, the fault event opens the circuit breakers to protect the cells.

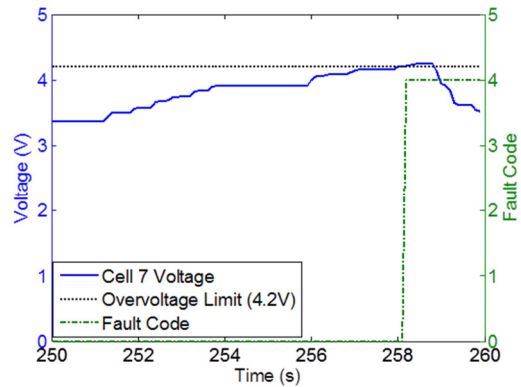


Figure 5. Over-voltage Battle Override. In Battle Override mode, over-voltage (> 4.2V) measured on any cell in the pack opens the circuit breakers.

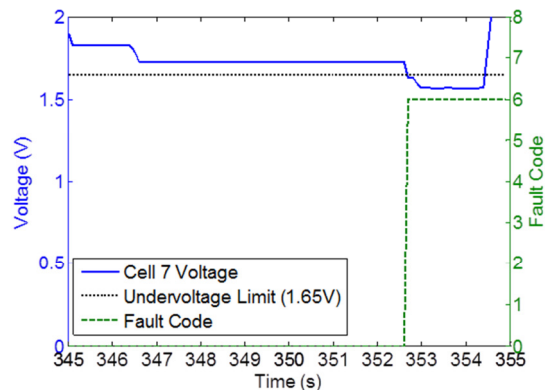


Figure 6. Under-voltage Battle Override. In Battle Override mode, under-voltage (< 1.65V) measured on any cell in the pack opens the circuit breakers.

The BMS has two overcurrent protection thresholds. The first is a hard limit to prevent extreme instantaneous charging currents from damaging the cells (set at 11A in our tests, but could be as high as safe operation will allow). The second is an integral criterion that supports high discharge rates over short periods of time to accommodate transient spikes, but activates pack protection if such high discharge currents continue for an extended period. The threshold used in our laboratory tests to prove the concept was 280 Coulombs over a 60s interval (this can be set via CAN to a desired value).

Figure 7 demonstrates this integral pack protection scheme. The first discharge pulse ( $7.7 < t < 63.7$  sec; 5A) activates the overcurrent protection fault (2) after 56 seconds corresponding to 280 Coulombs discharged over the 60-second period. After resetting the fault codes ( $t = 209$  sec), a second load of -4.55A is placed on the pack. After 60 seconds the total charge discharged is 275 Coulombs, which is below the threshold (recall that the figure is showing the integrated current over the last 60 seconds as opposed to integrated current over total time of operation). The pack remains loaded at -4.55A and the BMS never trips because the operation is away from the required 280 Coulombs limit. This example clearly demonstrates the implementation of the integral-based pack protection algorithm. It is important to stress that all safety protection limits are stored in non-volatile memory and can be changed or revised based on further tests and experiences. Other protection features were also tested and verified to activate once thresholds were crossed, including temperature limits.

**Cell Balancing Tests**

Figure 8 shows a laboratory test of the active cell balancing algorithm on the pack. Initially, the maximum voltage difference between the cells is approximately 70 mV, which is more than the allowed range of 10 mV. This difference was

created off-line by charging cells up to different SOC levels. After some time, active cell balancing brings the voltages closer to within half of that initial value. The intent of this result is to show that the active cell balancing approach converges and to show the robustness of the active cell balancing hardware, which was able to operate for long hours. The active cell balancing circuit can be easily modified to operate faster by using larger inductors and applying slower switching to the dual-power converters. The specific speed of cell balancing, however, depends on the application and the specific cells used.

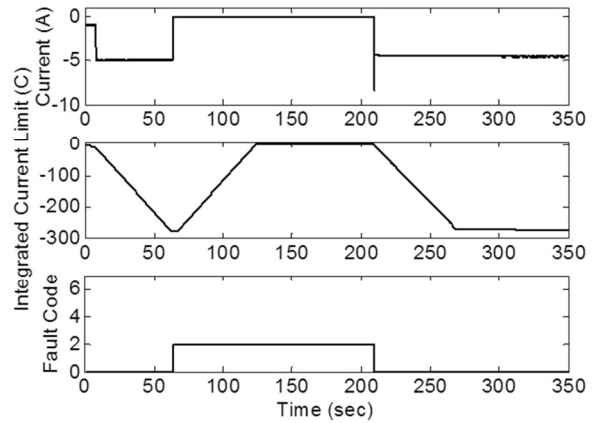


Figure 7. Over-charge protection based on 60s running window charge counter.

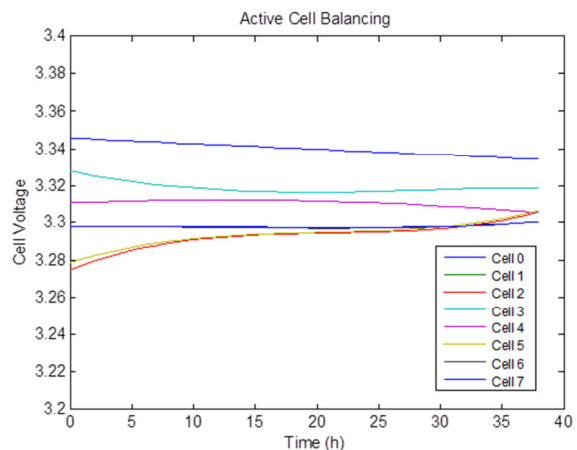


Figure 8. Cell voltages with active cell balancing.

### SOC Estimation Tests

In what follows we present results of SOC for the prototype +26.4VDC (i.e., +3.3VDC x 8), 60Ah 6T pack, comprised of twenty-four 20Ah lithium iron phosphate prismatic cells. Figure 9 shows pack terminal voltage and current during a charge at a 50A charge rate. The data shown was logged via CAN directly from the BMS. The pack was fully charged within 70 minutes, which agrees with the expected time for a charge of 50A into a 60Ah pack.

Figure 10 shows the pack terminal voltage as a function of SOC reported by the BMS over the same time period compared to the terminal voltage versus SOC computed using precise current measurement equipment and taken to be true SOC (it is referred to as Coulomb counter in the figures). The error between the true SOC and the BMS SOC is 1.88% on average over this period, as can be observed as well in Figure 11 where pack SOC is plotted versus time.

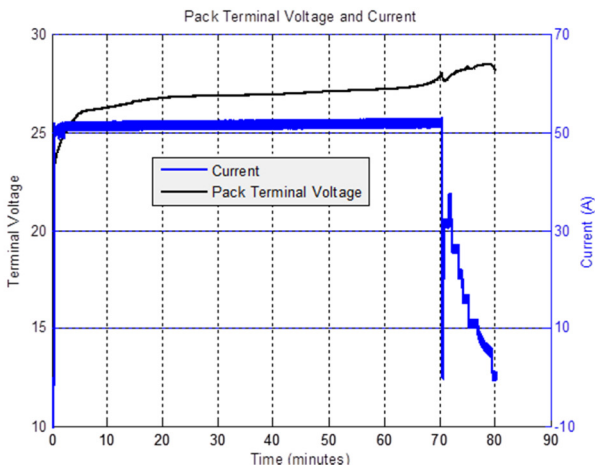


Figure 9. Pack terminal voltage and current while charging a 60Ah, +26.4VDC 6T pack (room temperature) at 50A.

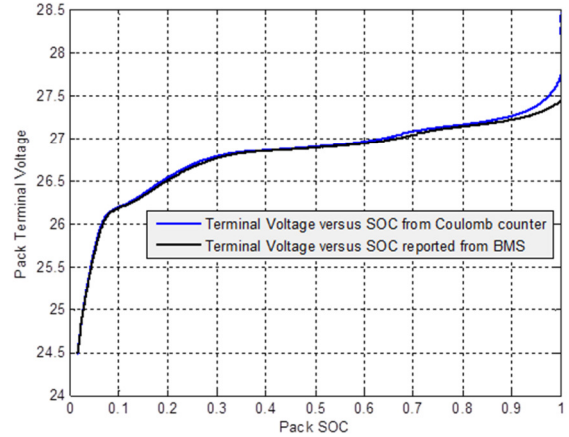


Figure 10. Pack terminal voltage vs. SOC while charging a 60Ah, +26.4VDC 6T pack (room temperature) at 50A.

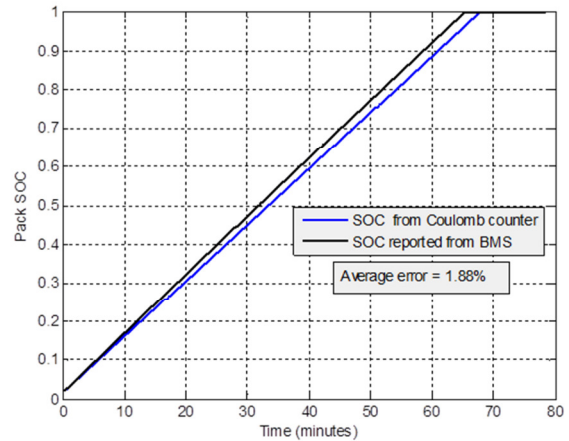


Figure 11. SOC reported by BMS while charging a 60Ah, +26.4VDC 6T pack (room temperature) at 50A.

Similarly, Figure 12 shows pack terminal voltage and current reported by the BMS CAN during a discharge of the 6T pack at 50A. The data shown were logged via CAN directly from the BMS. The pack was discharged within 70 minutes. Figure 13 shows the pack terminal voltage as a function of SOC as reported by the BMS, and compares this plot to the expected value based on the pack SOC computed by precise Coulomb counter method. Figure 14 shows the SOC reported while discharging the pack as a function of time. Charge taken out of the pack was 59Ah, which closely

agrees with the nominal capacity of the pack (i.e., 60Ah). The error in this case was 0.54% on average over the discharge period. SOC estimation at colder and warmer temperatures between -10°C and +45°C has shown average accuracies within 3% across full charge and discharge profiles [2].

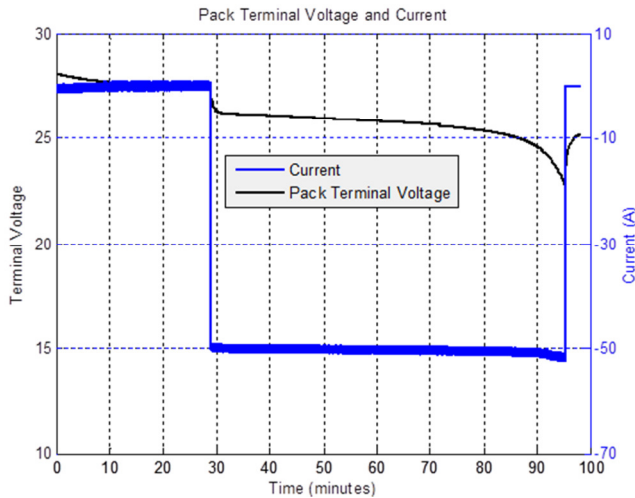


Figure 12. Pack terminal voltage and current while discharging a 60Ah, +26.4VDC 6T pack (room temperature) at 50A.

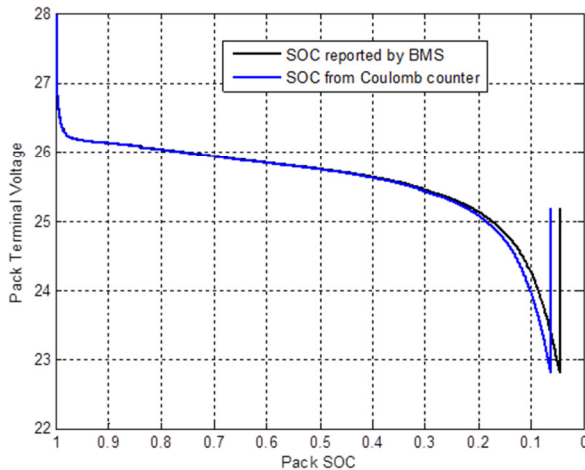


Figure 13. Pack terminal voltage vs. SOC while discharging a 60Ah, +26.4VDC 6T pack (room temperature) at 50A.

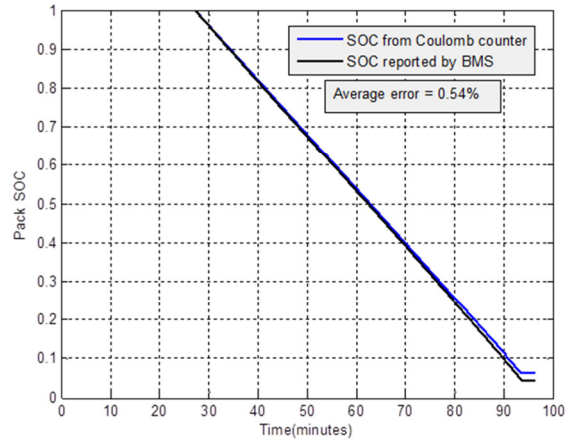


Figure 14. SOC reported by BMS while discharging a 60Ah, +26.4VDC 6T pack (room temperature) at 50A.

### SOH Estimation Tests

The critical part of the SOH algorithm is the estimation of internal resistance per super-cell in the pack. The resistance estimation from the BMS was tested and verified to be in agreement with off-line estimations performed using MATLAB<sup>®</sup>. To test the SOH algorithm, we introduced current steps to trigger the estimation of internal resistance (see the State of Health description under the Algorithm sub-section). We tested at different pack temperatures from +10°C to +30°C. Table 2 shows the result at +10°C. The nominal internal resistance of the prismatic cell used is 1mΩ at +10°C. The data in Table 2 show that the SOH estimation based on internal resistance is always better than 6%.

Super-Cell	Estimated Internal R (Ω)	Error (%)
1	0.001043	4.25
2	0.001013	1.28
3	0.001022	2.15
4	0.001059	5.90
5	0.001043	4.25
6	0.001007	0.68
7	0.001052	5.18
8	0.001022	2.23

**PA Tests**

The Power Availability algorithm was tested using the +26.4VDC, 60Ah 6T pack at room temperature. Figure 15 shows the power available in next 2 seconds and next 15 seconds as reported by the BMS integrated with the 6T pack.

To verify the BMS PA algorithm, we used an off-line calculation of power availability, which is shown in Figure 16. This calculated result agrees closely with the actual BMS result reported by the BMS in Figure 15. The reason for minor differences is that the theoretical result assumes all cells have the same impedance and voltage and with an internal resistance equal to the nominal value. The result from the BMS takes into account the exact value of cell internal resistance as measured on-line and the actual value of temperature.

**Engine Start Tests**

The high power density of lithium-based packs makes them an appealing source for vehicle engine starts. An engine start is characterized by short-duration current pulses on the order of hundreds up to one thousand amperes. We performed high-current tests on the +26.4VDC, 60Ah 6T pack integrated with the BMS. We were able to create a maximum load of 300A in the lab. Figure 17 shows the voltage and current as reported by the BMS when 300A were applied for approximately 2 minutes. Note the transitory behavior of the pack terminal voltage, which is considered in our model when estimating other metrics such as SOC.

In Figure 17 we see that the voltage drop at 42 seconds (when the load was connected), divided by the current difference, corresponds to a pack internal resistance of approximately 4 mΩ, which matches well with the nominal pack internal resistance in a new pack at room temperature of 5.3 mΩ (for a 8S3P pack).

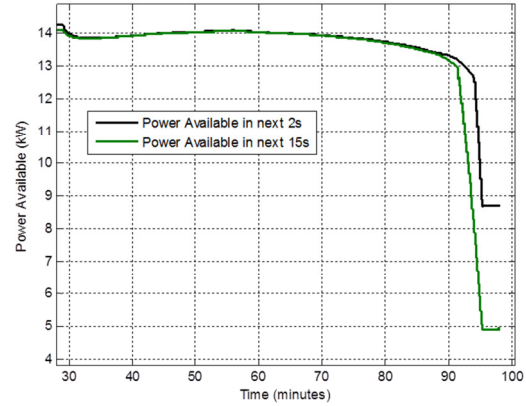


Figure 15. Power available of the +26.4VDC, 60Ah 6T pack as reported by the BMS.

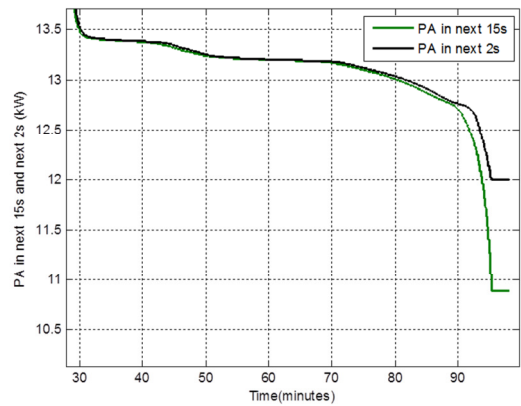


Figure 16. Theoretical (computed off-line) power available of the +26.4VDC, 60Ah 6T pack.

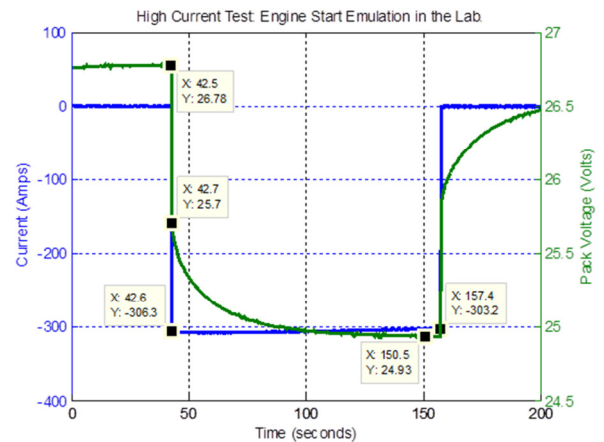


Figure 17. Voltage and current during a high current test.

The pack temperature measured by the BMS is shown in Figure 18 along with the SOC estimate during the test. The temperature during the discharge increased approximately 6°C. The SOC is in good agreement with our SOC estimate based on time, an independent current measurement. That is, the change in SOC was 17.1% according to our BMS (i.e., from 99.4% down to 82.3% as seen in Figure 18). A current of ~300 A was drawn out of the battery pack for 115 seconds. This is a charge of 9.8 Ah, which at the nominal pack charge of 19.2 Ah x 3 = 57.6 Ah represents a 17% drop in SOC. Determination of SOC at all times is critical to determine how many remaining engine starts can be delivered by a pack. It is straightforward to deduce that an engine start will reduce SOC by some amount to within some variance. This value can then be used to deduce the remaining engine starts available. Figure 19 shows the setup used in the laboratory for this high current test.

It is important to note that our BMS uses an innovative method to measure current. Our method is completely nonintrusive and eliminates the need for a current shunt or Hall Effect sensor, which pose problems such as increased internal impedance, space and volume challenges, and limited accuracy at low temperature. We have proven by test that our current sensor proves to be accurate to within 2% of a true current value obtained with additional equipment.

**FIELD TESTS**

We are currently in the process of evaluating the performance of the BMS and 6T pack with a U.S. Army ground combat vehicle.

This testing is expected to occur during the summer of 2013 and will include vehicle start and Silent Watch test profiles. Two +26.4VDC, 60Ah 6T packs will be installed in a ground combat vehicle and used to start the vehicle and run a Silent Watch profile. Results of these tests will be presented in a future paper.

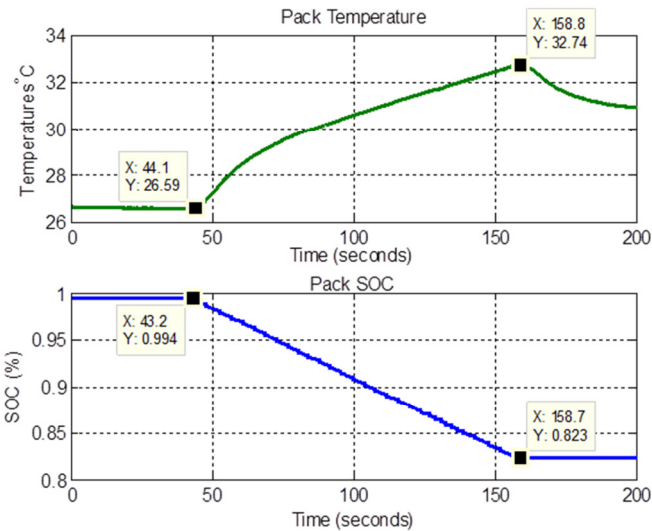


Figure 18. Pack temperature in °C and SOC(%).

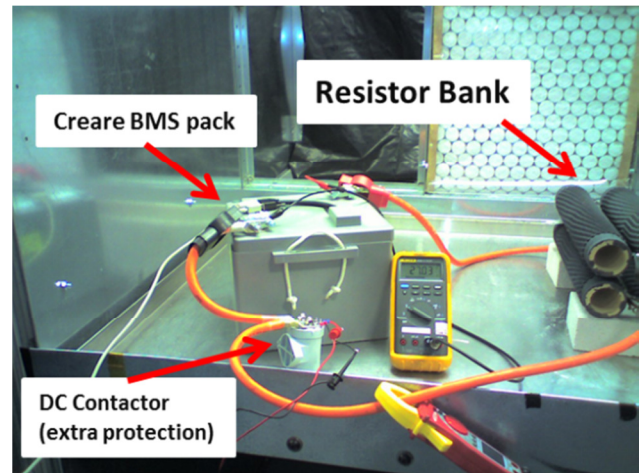


Figure 19. High current test laboratory setup.

## CONCLUSION

We have designed, implemented, and tested an advanced lithium-based Universal BMS integrated with a 6T pack.

Laboratory tests demonstrated that the advanced BMS is capable of accurate State of Charge, State of Health, State of Life, and Power Availability estimation, along with active and passive cell balancing, protection, and communication features in a wide range of thermal environments.

In the near future, the BMS will be integrated into a U.S. Army ground combat vehicle and tested. This field evaluation will raise the technology to TRL 6. The BMS represents a major step forward towards the incorporation of advanced lithium battery packs into U.S. Army and commercial vehicles.

## ACKNOWLEDGEMENTS

We would like to thank our sponsor, Mr. David Skalny, and his team at TARDEC for their continued support through this Small Business Innovation Research (SBIR) project.

## REFERENCES

- [1] Pilvelait, B., Rentel, C., Plett, G., Marcel, M., Carmen, D., “An Advanced Battery Management System for Lithium Ion Batteries,” *National Defense Industrial Association (NDIA) Ground Vehicle Systems Engineering and Technology Symposium*, Dearborn, Michigan, August, 2011.
- [2] Pilvelait, R., Rentel, C., Finger, W., Ruckman, L., Fogg, D., “Performance Results for a Universal Lithium Ion Battery Management System,” *National Defense Industrial Association (NDIA) Ground Vehicle Systems Engineering and Technology Symposium*, Dearborn, Michigan, August, 2012.
- [3] Plett, G., “Extended Kalman Filtering for Battery Management Systems of LiPB-based HEV battery packs. Part 2. Modeling and Identification,” *Journal of Power Sources*, Vol. 134, No. 2, August 2004, pp. 262–76.
- [4] Lee, W. C., Drury, D., Mellor, P., “Comparison of Passive Cell Balancing and Active Cell Balancing for Automotive Batteries,” *IEEE Vehicle Power and Propulsion Conference (VPPC)*, E-ISBN: 978-1-61284-246-2, Sept. 2011, pp. 1-7.